2013 IEEE/RSJ International Conference on
Intelligent Robots and Systems (IROS)
November 3-7, 2013. Tokyo, Japan

Off-road path tracking of a fleet of WMR with adaptive and predictive control

Audrey Guillet[1,3], Roland Lenain[1], Benoît Thuilot[2,3]
[1] Irstea, 24 avenue des Landais, 63172 Aubière, France
[2] Clermont Université, Université Blaise Pascal, Institut Pascal, BP 10448, 63000 Clermont-Ferrand, France
[3] CNRS, UMR 6602, Institut Pascal, 63171 Aubière, France
firstname.lastname@irstea.fr benoit.thuilot@univ-bpclermont.fr

***Abstract*— Off-road mobile robotics may have important interest in many fields of application such as agriculture or surveillance. In this paper, the control of a fleet of wheeled mobile robots, equipped with RTK-GPS sensors and communicating through WiFi, is investigated. The focus is particularly set on the control of a formation of several robots with respect to a reference trajectory, previously learned or computed off-line. Non-linear exact transformations permit to achieve a laterally and longitudinally decoupled model; from which the control of steering angle and velocity are derived separately in order to ensure the desired formation shape. Since the control of lateral distance to the reference trajectory is based on other works, only the longitudinal control is detailed in this paper. It is based on an adaptive and predictive control algorithm, in order to account for both sliding and actuator delays. The experimental results demonstrate the capabilities of the proposed approach.**

I. INTRODUCTION

Outdoor robotics is a challenging and promising area and responds to a real need [7], [1] as it permits to reach a better accuracy and therefore enhance the tasks to be achieved. If the use of a single robot may bring improvements, the collaboration of several autonomous vehicles permits to increase the area to be covered and the adaptability, pending on the application. Numerous researches have been carried out on control of a formation of robots [6], [9] (particularly in swarm robotics [3]). However, the control of the robots is based on the assumption of rolling without sliding and perfect actuators [5], [4]. This assumption is justified in the case of on-road applications and in structured environment, but it is not applicable in the off-road context addressed here. Indeed, the natural environment motion imposes some typical conditions such as low-grip, terrain irregularities, changes of soil texture, which leads to the necessity of taking into account for sliding in order to preserve accurate relative positioning [11]. To do so, an adaptive formation control algorithm is proposed, relying on an Ackermann model generalized to represent the effects of these uncertainties thanks to forces or sideslip angles [8], [12]. These parameters are estimated on-line through a model-based observer. The fleet is constituted in this application of several light robots, moving alongside a previously known trajectory. A robot is then positioned in the fleet with its lateral deviation (distance from the robot to the trajectory) and its longitudinal position (curvilinear abscissa) to the previous robot. Non-linear control techniques ensure that lateral servoing may be independent from longitudinal dynamics.

The contribution of this paper is in the development of a predictive algorithm coupled with a model-based adaptive control, in order to anticipate for longitudinal distance variation and consequently preserve the accuracy in the curvilinear distance between robots. The lateral control of a robot has been addressed in a previous work [10] and it will only be recalled.

This paper is organized as follows. First, the model of a robot dynamics is recalled in the context of a formation of several robots. After describing the observation of grip conditions, the lateral error regulation is presented and then, the longitudinal predictive control is detailed. This predictive approach, based on the predictive control strategy introduced in [13], estimates the future error (depending on the current robots state and the future shape of the trajectory), sets a desired future set point for each robot velocity and deduces the velocity control accounting for actuators delay and settling time. In the last part, full-scale experiments using two robots moving in natural environment are conducted and the results are analyzed to exhibit the contribution of the proposed algorithm.

II. MODELING OF A ROBOT

A. Extended kinematic model of a robot

Each robot of the fleet is modeled as a bicycle, like in the Ackermann model, composed of a fixed wheel at the center of the rear axle and a steering wheel at the center of the front axle. Given the considered off-road application in this work, it is impossible to assume, as classically, pure rolling without sliding. To account for sliding, two sideslip angles β_F and β_R are added: they are defined as the difference between the velocity vector direction at the center of each virtual wheel and the corresponding tire direction (see figure 1 and [11]).

Formation control is here investigated with respect to a known reference path Γ. As a result, each robot is modeled in the Frénet's frame.

The notations used in the sequel and shown in figure 1 are as follows:

- R is the center of the robot rear axle. It is the point to be controlled for each robot.
- F is the center of the robot front axle.

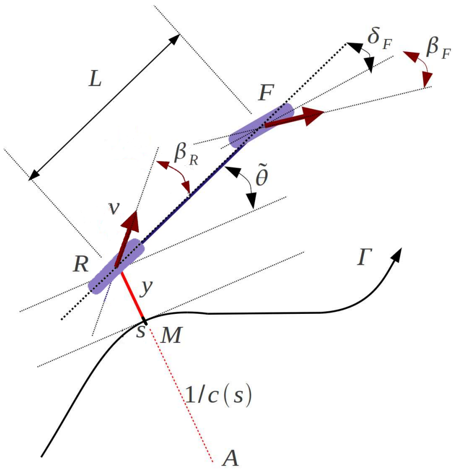

Fig. 1. Model of a robot in the Frénet's frame

- L is the robot wheelbase.
- s is the curvilinear coordinate of the closest point from R belonging to Γ. It corresponds to the distance covered along Γ by the robot.
- $c(s)$ denotes the curvature of path Γ at the abscissa s.
- y is the lateral deviation of the robot with respect to Γ.
- $\tilde{\theta}$ denotes the angular deviation of the robot to the tangent to Γ at the abscissa s.
- δ is the robot front wheel steering angle.
- v is the linear velocity of the robot at point R.
- β_F is the front sideslip angle.
- β_R is the rear sideslip angle.

Using these conventions, the extended kinematic model of the i^{th} robot of the fleet is established (further details are available in [11])

$$\left\{\begin{array}{lcl} \dot{s}_i & = & v_i \frac{\cos(\tilde{\theta}_i+\beta_i^R)}{1-c(s_i)\,y_i} \\ \dot{y}_i & = & v_i \sin(\tilde{\theta}_i+\beta_i^R) \\ \dot{\tilde{\theta}}_i & = & v_i \left(\cos\beta_i^R \frac{\tan(\delta_i+\beta_i^F)-\tan(\beta_i^R)}{L} - \frac{c(s_i)\ \cos(\tilde{\theta}_i+\beta_i^R)}{1-c(s_i)\,y_i}\right) \end{array}\right. \tag{1}$$

B. Linearization by chained system transformation

The extended kinematic model with sideslip angles keeps the same properties as the classical Ackermann model. Therefore, as it has been demonstrated in [14], the model (1) can be transformed into a chained system by invertible variables transformations.

$$\begin{array}{l} \begin{bmatrix} s_i \\ y_i \\ \tilde{\theta}_i \end{bmatrix} \rightarrow \begin{bmatrix} a_{1i} \\ a_{2i} \\ a_{3i} \end{bmatrix} = \begin{bmatrix} s_i \\ y_i \\ (1-c(s_i)\,y_i)\tan(\tilde{\theta}_i+\beta_i^R) \end{bmatrix} \\ \begin{bmatrix} v_i \\ \delta_i \end{bmatrix} \rightarrow \begin{bmatrix} m_{1i} \\ m_{2i} \end{bmatrix} = \begin{bmatrix} \dfrac{v_i\cos(\tilde{\theta}+\beta_i^R)}{1-c(s_i)\,y_i} \\ \dfrac{da_{3i}}{dt} \end{bmatrix} \end{array} \tag{2}$$

With these new state variables $a_{.i}$ and control variables $m_{.i}$, the system (1) becomes (3)

$$\left\{\begin{array}{lcl} \dot{a}_{1i} = \frac{d\,a_{1i}}{dt} & = & m_{1i} \\ \dot{a}_{2i} = \frac{d\,a_{2i}}{dt} & = & a_{3i}m_{1i} \\ \dot{a}_{3i} = \frac{d\,a_{3i}}{dt} & = & m_{2i} \end{array}\right. \tag{3}$$

Working in the Frénet's frame, it is interesting to derive the system with respect to the curvilinear abscissa (and not to the time anymore) as it permits to impose lateral control performances independent from time. With the notation $a'_{.i} = \frac{da_{.i}}{ds_i}$, the system (3) is turned into the 2-dimension linear system (4), as the first equation gives $a'_{1i} = 1$ and can then be removed from the system.

$$\left\{\begin{array}{lclcl} a'_{2i} & = & \frac{d\,a_{2i}}{ds_i} & = & a_{3i} \\ a'_{3i} & = & \frac{d\,a_{3i}}{ds_i} & = & m_{3i} = \frac{m_{2i}}{m_{1i}} \end{array}\right. \tag{4}$$

This transformation allows to separate longitudinal and lateral control since the dynamics of the state variables describing lateral motion (i.e. a_{2i} and a_{3i}) are independent from s_i. As a result, model (4) is used to design lateral control (i.e. the steering angle δ_i), whatever the robot speed v_i is; while the first equation of (1) is used to compute the longitudinal servoing (i.e. control the velocity v_i).

III. FORMATION CONTROL LAW

A. Formation control definition

In a fleet of n vehicles, to maintain the formation shape, each robot i has to converge to its desired lateral offset to the trajectory y_i^{des} and to its desired longitudinal interdistance to the previous robot d_i^{des}. The first robot, known as the leader, has only for command its desired lateral offset. These formation variables are illustrated in figure 2.
With these definitions, the formation control consists of maintaining the lateral and longitudinal variables of each robot to their desired values. The interdistance is computed alongside the trajectory, as the difference between the curvilinear abscissæ of the robots so that, even during the curves, the robots have always the same travel distance.

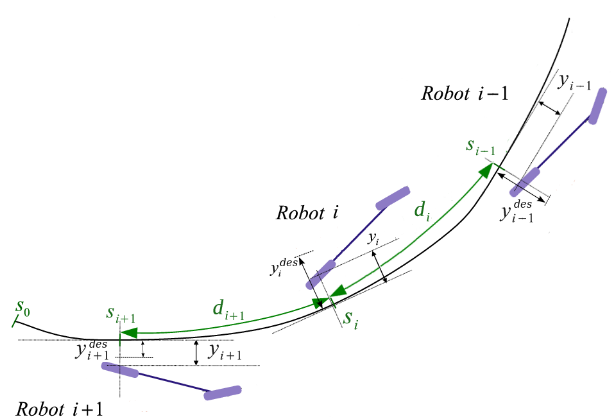

Fig. 2. Parameters of the robots in the fleet

Moreover, these parameters d_i^{des} and y_i^{des} are not necessarily constant and can be adapted to account for global positioning errors in the fleet or to handle specific situations such as the stop of a robot, the insertion or withdrawal of a robot in the fleet, obstacle avoidance, etc.

B. Sideslip angles observer

Control law design from model (1) requires the knowledge of the sideslip angles β_i^F and β_i^R. As it is very difficult to measure sliding with simple sensors, an observer is built to estimate on-line these angles. The algorithm principle of this observer is described in figure 3. It is based on the difference between the state computed with the estimated angles and the measured state. From the measured state $\bar{X}_i = [\bar{y}_i \ \ \bar{\tilde{\theta}}_i]^T$, the estimated sideslip angles are adapted through the observer law so that the state vector $X_i^{obs} = [y_i^{obs} \ \tilde{\theta}_i^{obs}]^T$ of model (1), regarded as an observed state, converges towards the measured state. Eventually, the sideslip angles (β_i^F, β_i^R) are adapted in the control law.
The details of the observer and the proofs of its performances are presented in [2].

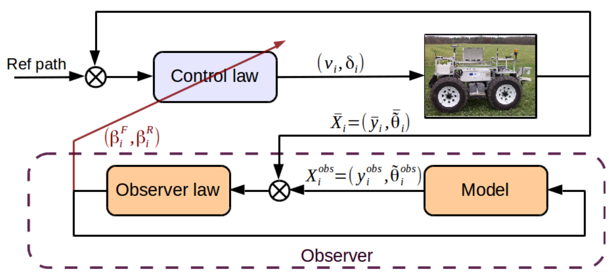

Fig. 3. Observer loop and adaptation of the sideslip angles

C. Servoing of the lateral distance

The objective of the control is to ensure the convergence of the lateral position y_i with respect to the trajectory to the desired offset y_i^{des}. From (2) and (4), it is equivalent to design the virtual control variable m_{3i} as $a''_{2i} = y''_i = m_{3i}$. Noting $\varepsilon_i^y = y_i - y_i^{des}$, a standard second order behavior is imposed by choosing:

$$m_{3i} = -K_d \varepsilon_i'^y - K_p \varepsilon_i^y + y_i''^{des} \qquad (K_d, K_p > 0) \tag{5}$$

From there, the expression of the steering angle δ_i is deduced (for the details, see [10])

$$\delta_i = \arctan\left[\tan(\beta_i^R) + \frac{L}{\cos(\beta_i^R)}\left(\frac{c(s_i)\cos\gamma_i}{\alpha_i} + \frac{A_i\cos^3\gamma_i}{\alpha_i^2}\right)\right] - \beta_i^F$$

$$\text{with: } \begin{cases} \gamma_i = \tilde{\theta}_i + \beta_i^R \\ \alpha_i = 1 - c(s_i)\, y_i \\ \eta_i = \tan\gamma_i - \dfrac{\dot{y}_i^{des}}{v_i\,\cos\gamma_i} \\ A_i = -K_p\,\epsilon_i^y - K_d\,\alpha_i\,\eta_i + c(s_i)\,\alpha_i\tan^2\gamma_i \end{cases} \tag{6}$$

Practically, the steering actuators have a non-null settling time which causes delays in the response and thus lateral errors, especially at high speed. To compensate for these errors, a predictive action is added. When the robot is satisfactorily positioned with respect to the reference path, the lock of the steering is mainly due to changes in the curvature of this reference path. Therefore, the lateral law (6) is split into two terms, in order to isolate the influence of the curvature of the trajectory:

$$\delta_i = \delta_i^{traj} + \delta_i^{deviation} \tag{7}$$

The δ_i^{traj} term is mainly dependent on the curvature $c(s_i)$ while the reactive part $\delta_i^{deviation}$ is not and consequently will not be modified by the prediction. Knowing the current state of the robot, it is possible to derive its future position after the settling time of the steering actuators, and as the reference trajectory is fully known, the curvature of the trajectory at this point and eventually the future steering angle value. A predictive algorithm then permits to design the control law ${\delta_i^{traj}}_{pred}$ leading to the future steering angle after the settling time of the actuators.
Eventually, the final lateral control law is obtained by adding the new predictive control part to the unchanged reactive part:

$$\delta_i = {\delta_i^{traj}}_{pred} + \delta_i^{deviation} \tag{8}$$

The details of this predictive algorithm for the lateral control law are available in [11].

D. Servoing of the longitudinal distance

The objective of the longitudinal control of the robot i consists of maintaining the curvilinear distance to the robot $i-1$ at its desired distance d_i^{des}.

1) Establishment of the velocity control law: Let ϵ_i be the interdistance error defined as the difference between the curvilinear abscissæ of both robots and the desired interdistance

$$\varepsilon_i = s_{i-1} - s_i - d_i^{des} \tag{9}$$

The desired interdistance characterize the formation shape and is defined by the supervisor so its evolution is known. Therefore, the derivation of the equation gives:

$$\dot{\varepsilon}_i = \dot{s}_{i-1} - \dot{s}_i - \dot{d}_i^{des} \tag{10}$$

Hence, according to the model (1), the desired velocity of the robot i is:

$$v_i = \frac{1 - c(s_i)y_i}{\cos(\tilde{\theta}_i + \beta_i^R)}\left(\frac{v_{i-1}\cos(\tilde{\theta}_{i-1} + \beta_{i-1}^R)}{1 - c(s_{i-1})y_{i-1}} - \dot{\varepsilon}_i - \dot{d}_i^{des}\right) \tag{11}$$

An exponential convergence of ε_i to 0 is desired:

$$\dot{\varepsilon}_i = -k_i\varepsilon_i \qquad (k_i \in R^{+*}) \tag{12}$$

This leads, in terms of control, to choose the virtual control variable m_{1i} (equal to $\dot{s}_i$, the velocity of the robot i along the curvilinear abscissa) as

$$m_{1i} = \dot{s}_{i-1} + k_i \varepsilon_i - \dot{d}_i^{des} \tag{13}$$

Reporting (12) in (11), the control law for the velocity of the i^{th} robot is:

$$v_i = \frac{1 - c(s_i) y_i}{\cos(\tilde{\theta}_i + \beta_i^R)} \left(\frac{v_{i-1} \cos(\tilde{\theta}_{i-1} + \beta_{i-1}^R)}{1 - c(s_{i-1}) y_{i-1}} + k_i \varepsilon_i - \dot{d}_i^{des} \right) \tag{14}$$

This control law ensures the exponential convergence of the i^{th} robot to the desired interdistance. Nevertheless, the settling time of the actuators is not anticipated here. This leads to overshoots in the response, especially during transient phases - at the start and when the longitudinal errors are significant. In order to limit, and even cancel, such overshoots, a predictive control is proposed to anticipate for low-level delay. Such a point of view requires the knowledge of the low-level model.

2) Modeling of the actuators behavior: The response of the robot to a velocity step control is recorded and identified as a second-order model. It can be described by the following discrete-state equations:

$$\begin{cases} X_{[n]}^{v_i} = A X_{[n-1]}^{v_i} + B v_{i\,[n-1]}^C \\ Y_{[n]}^{v_i} = C X_{[n]}^{v_i} \end{cases} \tag{15}$$

with $X_{[n]}^{v_i} = \begin{bmatrix} v_{i\,[n]}^R \\ v_{i\,[n-1]}^R \\ v_{i\,[n-1]}^C \end{bmatrix}$, $A = \begin{bmatrix} b_1 & b_2 & a_2 \\ 1 & 0 & 0 \\ 0 & 0 & 0 \end{bmatrix}$,

$$B = \begin{bmatrix} a_1 \\ 0 \\ 1 \end{bmatrix} \quad \text{and} \quad C = \begin{bmatrix} 1 & 0 & 0 \end{bmatrix}.$$

where v^R is the real velocity and v^C the control velocity. The parameters a_1, a_2, b_1, b_2 describe the behavior of the second-order and are specific to each robot in the fleet.

3) Predictive control: To design a predictive approach, a set point for the velocity must be derived, corresponding to the velocity to be reached after the prediction time t_h. This prediction time is chosen close to the settling time of the actuators. Indeed, the control computed at the instant t will be established at $t + t_h$. As the state of the robots will have changed, it seems relevant to estimate at time t the state of the robots at the instant $t + t_h$ in order to compute this predictive velocity term. That way, at $t + t_h$, the control sent will be really corresponding to the current state.

Knowing the velocities (and the states) of the robots $i - 1$ and i at the instant t, it is possible to extrapolate on the future position of both robots at $t + t_h$.

$$\begin{aligned} s_i(t + t_h) &= s_i(t) + t_h . \dot{s}_i(t) \\ &= s_i(t) + t_h \frac{v_i \cos(\tilde{\theta}_i + \beta_i^R)}{1 - c(s_i)\, y_i} \end{aligned} \tag{16}$$

As a result, the estimated future interdistance error $\varepsilon_i(t + t_h)$ can be deduced:

$$\varepsilon_i(t + t_h) = s_i(t + t_h) - s_{i-1}(t + t_h) - d_i. \tag{17}$$

Furthermore, the curvature of the trajectory at $s_i(t + t_h)$ can also be deduced since Γ is known.
In the control law (14), the rear sideslip angles β^R and the angular deviation $\tilde{\theta}$ of the robots can not be predicted. However, in practice, during path tracking, these angles stay slowly varying during the prediction time t_h. Thus, their future values can be taken as equal to their actual values without significant errors.
As for the lateral offsets of the robots, they are considered as being slowly varying during the prediction interval and their future values are approximated to their actual values.
The last parameter to be estimated is the velocity v_{i-1} of the robot to be followed, chosen as the control sent to the actuators at the instant t, which will be the real velocity after the prediction time.
As a result, the set point for the velocity is derived as:

$$\begin{aligned} v_i^{obj} \;&=\; v_{i-1}^C \frac{1 - c(s_i(t + t_h)) y_i}{1 - c(s_{i-1}(t + t_h)) y_{i-1}} \frac{cos(\tilde{\theta}_{i-1} + \beta_{i-1}^R)}{\cos(\tilde{\theta}_i + \beta_i^R)} \\ &\quad + \frac{1 - c(s_i(t + t_h)) y_i}{\cos(\tilde{\theta}_i + \beta_i^R)} k_i \varepsilon_i (t + t_h) \end{aligned} \tag{18}$$

From the velocity v_i of the i^{th} robot at instant t, a desired shape can be defined to reach v_i^{obj} at t_h. An integer n_h is set as the number of iterations to reach t_h and chosen as the desired number of points of coincidence between t and t_h. With this notation, the iteration of calculation n corresponds to the present time t and the iteration $n + n_h$ to the prediction time $t + t_h$. In this application, a first order shape is chosen as:

$$v_{i\,[n+j]}^{des} = v_i^{obj} - \mu^j (v_i^{obj} - v_{i\,[n]}^R) \tag{19}$$

for $j \in [0, n_h]$.

where $\mu \in [0, 1[$ is a parameter regulating the convergence speed to the objective.

From this desired shape response, the control velocities $v_{i\,[n+j]}^C$ are sought, for which the response of the low-level model will be the closest to the desired velocity $v_{i\,[n+j]}^{des}$ at each iteration. To do so, a criteria $D(n)$ is defined as the sum of the square of the difference between the predicted response velocity $\hat{v}_i^R$ and the desired velocity v_i^{des}.

$$D(n) = \sum_{k=0}^{n_H} (\hat{v}_{i\,[n+k]}^R - v_{i\,[n+k]}^{des})^2 \tag{20}$$

The minimization of this criteria gives the optimal sequence of controls $[v_{i\,[n]}^C, ..., v_{i\,[n+n_H]}^C]$. From this sequence, the first term is kept as the new velocity control to be applied to the robot.

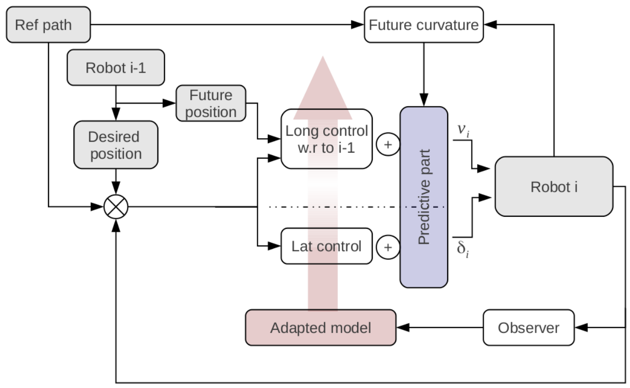

Fig. 4. Principle of the overall formation control algorithm

Overall algorithm

The overall algorithm for the control of the formation is depicted in figure 4. The robots are positioned with respect to the reference path and the lateral and longitudinal controls of one robot are computed independently. The proposed contribution takes place in the longitudinal part, in which the algorithm does not use only the current position of the robot but also the future positions of the considered robot i and the reference robot $i-1$ to establish the desired velocity after the settling time of the actuators. Eventually, the predictive part accounts for the low-level dynamics and derives the control values sent to the vehicle.

IV. Experimental results

A. Experimental platforms

The experiments have been carried out with a fleet of two vehicles depicted in figure 5. The two platforms are four independently-driven wheeled robots, with an identical wheelbase of 1.2 m. The leader robot (on the right of the picture) can go up to 8 m/s for a weight of 420 kg while the follower robot weights 650 kg for a maximum velocity of 4 m/s. They are fitted with electrical actuators whose characteristics are as follows: the settling times of the driving motors for the leader and the follower robots are respectively $1.0s$ and $1.5s$; the response times of the steering actuators are $0.4s$ for the leader and $0.6s$ for the follower.

Fig. 5. The mobile robots

Regarding the sensors, the robots are fitted with an on-board RTK-GPS receiver providing a position accurate within 2 cm at a sampling rate of 10 Hz. The communication between the robots is ensured through a WiFi module.

B. 2-robots fleet trajectory tracking results

The path followed by the robots has been recorded during a previous manual driving (and the trajectory thus generated has been better specified by an off-line interpolation of the 10 Hz GPS points). The reference trajectory, presented in the figure 6, is composed of a flat grass-covered soil, with two crossings of a shelly sand path.

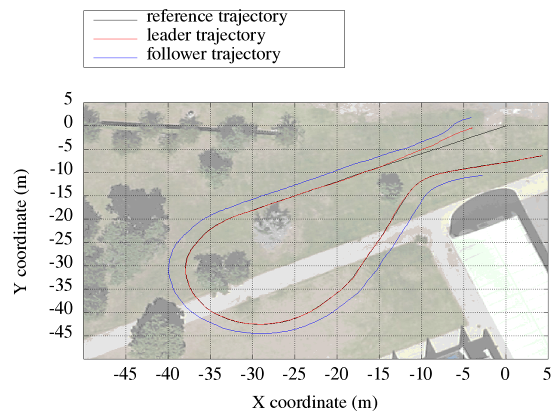

Fig. 6. Reference and real trajectories followed by the robots

During path tracking operations, the leader has to follow the reference trajectory ($y_1^{des} = 0$) at a variable desired speed and the follower has to be controlled with a desired lateral distance of 2 m to the trajectory and a longitudinal interdistance of 9 m with the leader.
On the first third of the trajectory (from 0 to 33 m), the desired velocity for the leader is constant at 2 m/s then, from 33 to 65 m, the desired velocity decreases at 1.5 m/s before going back at 2 m/s on the last part of the path, as can be seen on the black curve in the figure 10.

The path tracking results for the lateral servoing are presented in figure 7. It can be seen that the lateral control of the robots to their desired lateral offset to the trajectory is ensured with a maximal error of $0.2\ m$. In particular, it can be noted that the curvature changes in the reference path do not degrade the quality of the servoing.

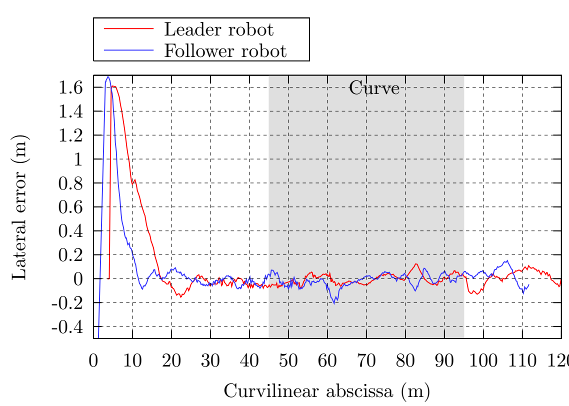

Fig. 7. Lateral error of the robots during the path tracking

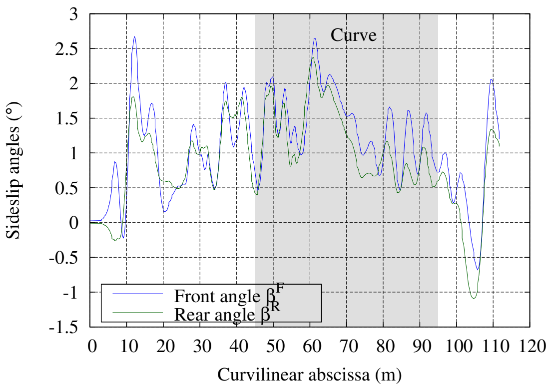

Fig. 8. Front and rear sideslip angles of the follower robot

The sideslip angles (β^F, β^R) are also recorded and are shown to be non-negligible, as can be seen in figure 8 where the sideslip angles of the follower robot are presented. Indeed, at the more curved part of the trajectory (the abscissa 60 m), the observed angles are about $2\,°$. If the sliding had not been taken into account, and given the wheelbase of the robot, this would have led to lateral deviation of $0.4\ m$, which is twice the precision obtained for the lateral control. More results on the pertinence of adding the sideslip angles in the model are available in [11].

The longitudinal law was meant to regulate the interdistance and the results are presented in figure 9. The control without any prediction (in green line in the figure 9) consists of imposing the control law (14) while the proposed predictive control ($v^C_{i\,[n]}$ of the section III-D.3) leads to the interdistance error presented in blue line in the figure 9.

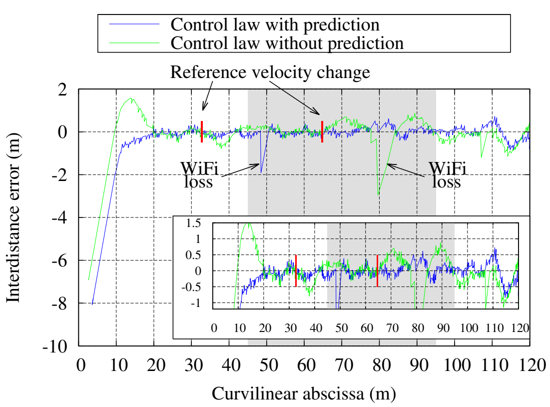

Fig. 9. Interdistance error of the follower with respect to the leader

At the start, the robots are approximately side by side so the longitudinal error is important. If the low-level delay is not taken into account, the follower robot converges to the desired interdistance with an overshoot of 1.5 m. The proposed predictive algorithm accounts for this low-level dynamics and permits to suppress this overshoot. This improvement is reflected in the figure 10 where the transient phases are taken into account more quickly, and the resulting velocity controls are sent earlier with the prediction module.

In parallel, the figure 10 presents the velocity control sent to the actuators during the same path tracking for the two compared approaches.

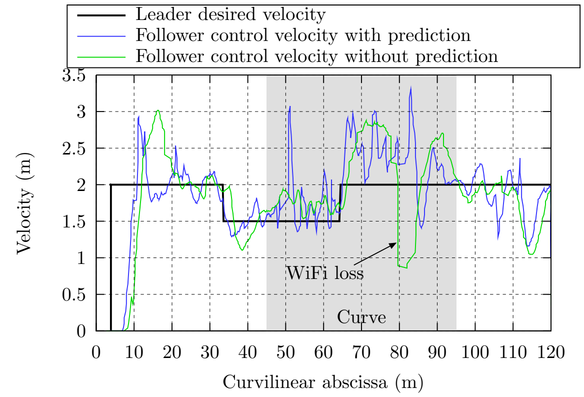

Fig. 10. Velocity control sent during the path tracking

From the abscissa 0 to 45 m, the robots are on a straight line so the velocity of the follower converges to the desired velocity of the leader. After, the robots track the left curve so, the follower being on the outside of the curve, its velocity increases to follow the leader. Eventually, the last part of the trajectory (from abscissa 110 m) is curved on the right so the leader is inside the curve and slows down.

The results show that, after the starting part, the longitudinal error stays between $\pm 0.3\ m$ and neither changes in path curvature nor changes in reference velocity create interdistance error, contrary to the non-predictive law which creates non negligible overshoots, up to $0.8\ m$. This is reflected, in figure 11, by the standard deviation which is divided by 3, to less than 20 cm with the proposed approach while the error is centered on 0.

	Without prediction	With prediction
Mean	-8.0 cm	-0.2 cm
Std	44.7 cm	16.6 cm

Fig. 11. Properties of the path tracking results for the interdistance error

These overshoots can be dangerous in a fleet of robots if the desired interdistance between the robots is small, e.g. less than 2 m. On the other hand, the convergence without overshoot of the proposed law is very interesting in the case of a fleet of numerous robots where one is longitudinally positioned with reference to the previous robot as it should reduce the oscillation effects and error accumulation frequently observed.

As can be seen in figure 9, losses of WiFi communication from the leader to the follower have been experienced during the experiments (curvilinear abscissæ 48 m for the control with prediction, 80 m for the algorithm without prediction). In that case, the follower keeps the last values received for the computation of the control ; that is why the interdistance, and thus the velocity, decreases. When the communication is restored, the follower performs as at the start, converging to the desired interdistance with overshoot when there is no prediction and without overshoot in the case of the proposed algorithm.

V. Conclusion and future work

This paper addresses the formation control of several wheeled mobile robots in off-road conditions, based on the path tracking formalism. Thanks to an adaptive and predictive approach, specificities of off-road motion can be accounted in order to preserve a high level of accuracy, whatever grip conditions, the desired global motion and the actuators settling times. In particular, the anticipation of robots positions, thanks to on-line sideslip angles estimation allows to design a model predictive control, which decouples longitudinal and lateral dynamics. As a result, steering angle and velocity control are separately addressed. This permits to control independently a relative curvilinear distance and a lateral offset between robots to desired set points.

Particularly focused on the longitudinal control, this paper demonstrate the capabilities of predictive longitudinal control to prevent the curvilinear distance between robots from overshoots due to actuator settling time and wheels slippage, while lateral performances are comparable to results obtain in previous work on path tracking results. Lateral relative position is indeed accurate within few centimeters, while the maximal longitudinal distance error reached during full scale experiments decreases from almost 2 m (when using classical approaches) to 0.3 m (when using the predictive control proposed in this paper). Such a gain in accuracy is particularly crucial when robots moves closely or are subjected to speed variations. Indeed, important overshoots may lead to hazardous situations (collisions) and does not permit to preserve a formation. On the contrary, the control framework proposed in this paper allows to investigate cooperative tasks (such as cooperative transportation).

These results have been obtained on two mobile robots using only RTK-GPS as exteroceptive sensors and wireless communication devices. As it can be seen on during experiments, such an equipment is subjected to possible communication losses, or decrease in GPS localization accuracy. If the proposed control is robust to short "cut", a long signals unavailability may lead to dangerous situations. The addition of new exteroceptive sensors or the prediction of robots positions may permits to overcome such difficulties. Moreover, if simulations have permitted to validate the control structure to formation control of four mobile robots, actual results have to be extended to a larger number of robots (limited to two in this paper).

Acknowledgments

This work has been sponsored by the French government research program Investissements d'avenir through the RobotEx Equipment of Excellence (ANR-10-EQPX-44) and the IMobS3 Laboratory of Excellence (ANR-10-LABX-16-01), by the European Union through the program Regional competitiveness and employment 2007-2013 (ERDF Auvergne region), by the Auvergne region and by French Institute for Advanced Mechanics

References

[1] S. Blackmore, B. Stout, M. Wang, and B. Runov, *Robotic agriculture - the future of agricultural mechanisation?*, 5th European Conference on Precision Agriculture (ECPA), Upsala (Sweden) (2005).

[2] C. Cariou, R. Lenain, B. Thuilot, and M. Berducat, *Automatic guidance of a four-wheel-steering mobile robot for accurate field operations*, Journal of Field Robotics **26** (2009), no. 6-7, 504–518.

[3] E. Şahin, *Swarm robotics: From sources of inspiration to domains of application*, Swarm Robotics (E. Şahin and W. M. Spears, eds.), Lecture Notes in Computer Science, vol. 3342, Springer Berlin Heidelberg, 2005, pp. 10–20.

[4] A. De Luca, G. Oriolo, and M. Vendittelli, *Control of wheeled mobile robots: An experimental overview*, RAMSETE: Articulated and Mobile Robotics for Services and Technology (2001), 181–226.

[5] C. C. De Wit, G. Bastin, and B. Siciliano, *Theory of robot control*, Springer-Verlag New York, Inc., 1996.

[6] J.P. Desai, J. Ostrowski, and V. Kumar, *Controlling formations of multiple mobile robots*, IEEE International Conference on Robotics and Automation (ICRA), Leuven (Belgium), 1998.

[7] K. Iagnemma and S. Dubowsky, *Mobile robot rough-terrain control (RTC) for planetary exploration*, Proceedings of the 26th ASME Biennial Mechanisms and Robotics Conference, DETC, 2000.

[8] G. Ishigami, K. Nagatani, and K. Yoshida, *Slope traversal controls for planetary exploration rover on sandy terrain*, Journal of Field Robotics **26** (2009), no. 3, 264–286.

[9] G. Klančar, D. Matko, and S. Blažič, *A control strategy for platoons of differential drive wheeled mobile robot*, Robotics and Autonomous Systems **59** (2011), no. 2, 57 – 64.

[10] R. Lenain, J. Preynat, B. Thuilot, P. Avanzini, and P. Martinet, *Adaptive formation control of a fleet of mobile robots: Application to autonomous field operations.*, IEEE International Conference on Robotics and Automation (ICRA), Anchorage (Alaska), 2010.

[11] R. Lenain, B. Thuilot, C. Cariou, and P. Martinet, *High accuracy path tracking for vehicles in presence of sliding: Application to farm vehicle automatic guidance for agricultural tasks*, Autonomous Robots **21** (2006), 79–97.

[12] N. Noguchi, J. Will, J. Reid, and Q. Zhang, *Development of a master–slave robot system for farm operations*, Computers and Electronics in agriculture **44** (2004), no. 1, 1–19.

[13] J. Richalet, A. Rault, J.L. Testud, and J. Papon, *Model predictive heuristic control: Applications to industrial processes*, Automatica **14** (1978), no. 5, 413 – 428.

[14] C. Samson, *Control of chained systems application to path following and time-varying point-stabilization of mobile robots*, IEEE Transactions on Automatic Control **40** (1995), no. 1, 64 –77.